XLIII SEMANA NACIONAL DE ENERGÍA SOLAR 2019
NUEVO VALLARTA, NAYARIT del 14 al 18 OCTUBRE
Energía sustentable: una necesidad
ANES Asociación Nacional de Energía Solar

Evaluation of natural ventilation using age of air

Sonny F. Díaz-Calderón[a], J. Antonio Castillo[b] y Guadalupe Huelsz[a]
a) Instituto de Energías Renovables, Universidad Nacional Autónoma de México, A. P. 34, 62580 Temixco, Mor., México, Tel/Fax 55+56-22-97-41, **sfdc@ier.unam.mx**
b) Departamento de Arquitectura y Diseño, Universidad de Sonora, Blvd. Encinas y Rosales, Col. Centro, 83000, Hermosillo, Son., México, Tel 66+22-59-21-79.

RESUMEN

En este trabajo se presenta la evaluación de la ventilación natural en una edificación con ventilación cruzada, usando parámetros asociados a la edad del aire en simulaciones de dinámica de fluidos computacional (CFD, por sus siglas en inglés) con un modelo de turbulencia RANS. Los parámetros asociados a la edad del aire son utilizados para la evaluación de la calidad del aire al interior de edificaciones. La edad del aire es el tiempo que una parcela de moléculas de aire ha permanecido al interior de la edificación a partir de que entró por una de las aperturas de la edificación. Los parámetros asociados a la edad del aire son la edad local promedio del aire y la edad espacial promedio, con ellos se calcula la eficiencia de ventilación. Se presenta la metodología para el cálculo de estos parámetros utilizando el software de CFD ANSYS Fluent. Se utiliza un modelo numérico validado experimentalmente a escala de laboratorio (1/15). Se realizan simulaciones a dos escalas de la edificación, escala laboratorio y escala real, donde se mantienen similitud geométrica, cinemática y dinámica. Se obtiene el tiempo característico de cada escala y se demuestra que los parámetros asociados a la edad del aire normalizados con el tiempo característico son iguales en ambas escalas. Se incluye una comparación de los parámetros asociados a la edad del aire con otros parámetros empleados para la evaluación de la ventilación natural.

ABSTRACT

This paper presents the evaluation of natural ventilation in a building with cross ventilation using parameters associated with age of air in computational fluid dynamics (CFD) simulations with a RANS turbulent model. The parameters associated with the age of air are used for air quality evaluation inside buildings. The age of the air is the time that a parcel of air molecules has stayed inside the building since it has entered through one of the building openings. The parameters associated with the age of air are the local mean age of air and the spatial average of the age. With these two parameters, the ventilation efficiency is obtained. The calculation methodology for the parameters is presented using ANSYS Fluent CFD software. A numerical model experimentally validated with a laboratory scale model (1/15) is used. Simulations are carried out for two scales of the building, laboratory scale and full scale, maintaining geometric, kinematic and dynamic similarities. The characteristic time of each scale is obtained and it is demonstrated that the parameters normalized with the characteristic time have the same value in both scales. A comparison of the parameters associated with the age of air with other parameters commonly used for the evaluation of natural ventilation is included.

Palabras clave: Natural ventilation; Cross-ventilation; Age of air; Computational fluid dynamic; CFD; RANS; Coupled simulation.

INTRODUCTION

In studies of natural ventilation in buildings, the use of age of air [s] and air exchange rate I [s^{-1}] as evaluation parameters is reported (Jin et al., 2016; Montazeri and Montazeri, 2018). The age of air is defined as the time that a parcel of air has stayed inside the building since it has entered through one of the building openings (Etheridge and Sandberg, 1996). I is defined as the inverse of nominal time constant ($I = \tau_n^{-1} = Q/V$), where Q [m^3/s] is the volumetric flow rate across the openings of the building and V [m^3] the interior air volume. The inverse of I is known as the air changes per time unit (ASHRAE, 2015). By definition, I does not consider the air distribution, *i.e.* the inlet jets, recirculation zones and stagnation points. While the residence time does consider the air distribution inside the building, due to its definition as the average of the age of air in the exhausts. To implement the parameters associated with the age of air in studies of natural ventilation, the Group of Energy in Buildings at IER-UNAM develops a methodology using CFD simulations. Thus in this work, the methodology implementation on cross ventilation cases is presented.

AGE OF AIR THEORY

In this section a summary of the age of air theory by Etheridge and Sandberg (1996) is presented. In the age of air analysis, three periods of times are defined: internal age τ_i [s], residual lifetime τ_{rl} [s] and residence time τ_r [s] . τ_i is the time that a parcel of air inside the building has elapsed in the building since its entrance, τ_{rl} is the remaining time that a parcel of air will spend in the building until its leaving and τ_r is the time when a parcel of air leaves the room, *i.e.* is the sum of the internal age and the residual lifetime

$$\tau_i + \tau_{rl} = \tau_r \quad [s] \tag{1}$$

Since ventilation is a turbulent flow problem, these three periods of time are represented as frequency distributions and their averages can be calculates in two ways. The local average $\bar{\tau}$ is the average of ages of the air molecules in a parcel and the spatial average $\langle\tau\rangle$ is the average of all local ages of the air volume. In studies of natural ventilation, the calculation of local mean age of air $\bar{\tau}_i$, spatial average of age of air $\langle\tau_i\rangle$ and spatial average of residence time $\langle\tau_r\rangle$ are relevant. The transport equation for $\bar{\tau}_i$ is

$$\left(\overline{u}\frac{\partial\overline{\tau_i}}{\partial x}+\overline{v}\frac{\partial\overline{\tau_i}}{\partial y}+\overline{w}\frac{\partial\overline{\tau_i}}{\partial z}\right)-\frac{\partial}{\partial x}\left(D_{ex}\frac{\partial\overline{\tau_i}}{\partial x}\right)-\frac{\partial}{\partial y}\left(D_{ey}\frac{\partial\overline{\tau_i}}{\partial y}\right)-\frac{\partial}{\partial z}\left(D_{ez}\frac{\partial\overline{\tau_i}}{\partial z}\right)=1, \quad (2)$$

where D_{ex}, D_{ey} and D_{ez} are the effective diffusion coefficients on each coordinate axis.

From the principle of mass conservation, two relationships between the ages in the interior of the building and the ages in the exhausts of the building are deduced. The first relationship is between the spatial average of residence time and the spatial average of age of air

$$\langle\tau_r\rangle = 2\langle\tau_i\rangle. \quad (3)$$

$\langle\tau_r\rangle$ can be interpreted as the time that the air volume is removed. The second relationship is the average of residence time across the total exhaust area $\overline{\tau_r}$ and is equal to the nominal time constant

$$\overline{\tau_r}\Big|_e = \tau_n = \frac{V}{Q}. \quad (3)$$

The ideal piston flow is the most effective form of ventilation. This flow is unidirectional where the diffusive terms are considered equal to zero. Thus, this case has the minimum value of $\langle\tau_i\rangle$, $\langle\tau_i\rangle_{min}$, the minimum value of $\langle\tau_r\rangle$, $\langle\tau_r\rangle_{min}$, and they can be expressed as

$$\langle\tau_i\rangle_{min} = \frac{\tau_n}{2} \quad \text{and} \quad \langle\tau_r\rangle_{min} = \tau_n. \quad (4) \text{ and } (5)$$

The ventilation efficiency ϵ is defined as

$$\epsilon = 100\frac{\langle\tau_i\rangle_{min}}{\langle\tau_i\rangle}. \quad (6)$$

Then, ϵ can be also expressed as

$$\epsilon = 100\frac{\langle\tau_r\rangle_{min}}{\langle\tau_r\rangle} = \frac{\tau_n}{2\langle\tau_i\rangle}. \quad (7)$$

APPLICATION CASE

The application case is an isolated building in full scale with two opposite axial openings, *i.e.* cross-ventilation case. The dimensions of the building are 4.50 m × 4.50 m × 2.25 m (width × length × height) and of the openings are 0.90 m × 0.45 m (width × height). The building Reynolds number of the case is $Re_b = U_{ref}y_{ref}/\nu = 6.69\times10^4$ with a reference velocity U_{ref} = 0.47 m/s taken at the height of the building y_{ref} = 2.25 m and air kinematic viscosity ν. The atmospheric boundary layer is calculated with the power law $U(y) = U_{ref}(y/y_{ref})^{\alpha}$ with an exponential constant α = 0.25, corresponding to a sub-urban region.

CFD VALIDATION

For the validation of the CFD simulations, the experimental results obtained by Kurabuchi et al. (2004) are used. 3D steady RANS equations with a turbulence model are performed using the commercial code ANSYS Fluent 19 (ANSYS, 2019). The experiment is performed in a wind tunnel with a scale model, measuring the central plane of the model with the Particle Image Velocimetry (PIV) technique. The geometric, dynamic and kinematic similarities (Moonen et al., 2012) are conserved in the experiments. The model is scaled 1/15. The reference velocity U_{ref} = 7.0 m/s is taken at the height of the experimental model y_{ref} = 0.15 m. Figure 1 shows the experimental model and its dimensions.

The dimensions of the domain are 1.8 m × 3.0 m × 0.9 m (width × length × height). The upstream and the downstream lengths are 3 × y_{ref} and 15 × y_{ref}, respectively. From the lateral walls and the roof of the building to the corresponding parallel walls of the domain have a distance of 5 × y_{ref} (Fig. 2).

The mesh of the domain is built with the surface grid extrusion technique (van Hooff and Blocken, 2010). The mesh is block-structured with hexaedric cells. An aspect ratio of 20% is used for the increment in size between cells. A reference case is created with a total of 579,246 cells (mesh 2) (Fig. 2).

The inlet conditions are taken from the experimental measurements of velocity and turbulent kinetic energy. The velocity profile *U(y)* is calculated with the logarithmic law,

$$U(y) = \frac{u^*_{ABL}}{\kappa}\ln\left(\frac{y+y_0}{y_0}\right), \quad (7)$$

where u^*_{ABL} = 0.75 m/s is the atmospheric boundary layer friction velocity, κ = 0.42 is the von Karman constant, y_0 = 0.0027 m is the roughness length and y is height coordinate. The turbulent kinetic energy (TKE) profile *k(y)* is defined by the standard deviation of the velocity obtained in the experimental measurements,

$$k(y) = \sigma_x^2(y). \quad (8)$$

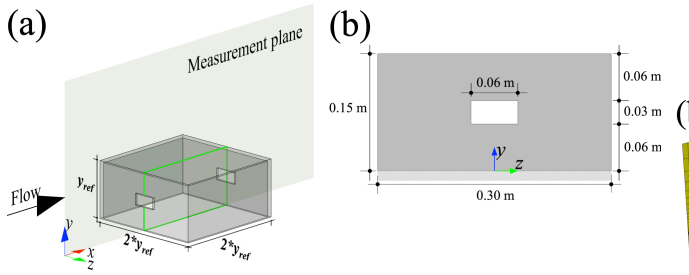

Figure 1: Scale model of the building with two openings: (a) isometric view of the model with its measurement plane; (b) front view of the model with dimensions.

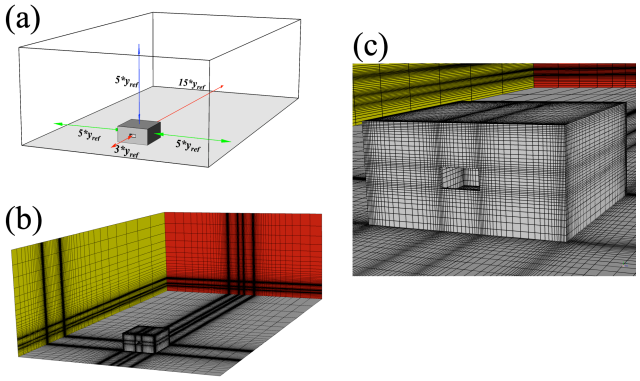

Figure 2: Computational domain of the building, isometric view of: (a) dimensions of the domain; (b) entire domain and (c) detail of the building with 579,246 cells.

The turbulent dissipation rate (TDR) and the specific dissipation rate (SDR) profiles, $\varepsilon(y)$ and $\omega(y)$ respectively, are calculated by

$$\varepsilon(y) = \frac{u_{ABL}^{*3}}{\kappa(y + y_0)}, \quad \omega(y) = \frac{\varepsilon(y)}{C_\mu k(y)}, \tag{9), (10}$$

where $C\mu = 0.09$ is an empirical constant (Tominaga et al., 2008).

Standard wall functions (Launder and Spalding, 1974) are used for the ground and room surfaces with roughness modification (Cebeci and Bradshaw, 1977). For ANSYS-Fluent the values of the sand-grain roughness height k_s and the roughness constant C_s must be given. For ground surface, k_s is calculated using (Blocken et al., 2007b)

$$k_s = \frac{9.793 y_0}{C_s}, \tag{8}$$

considering $C_s = 7.0$ that gives $k_s = 0.0039$ m. For the model surfaces, $k_s = 0$ and $C_s = 0.5$ are fixed, which represent smooth surfaces. Conditions of symmetry are used in lateral and top boundaries of the domain and zero static pressure is applied at the outlet boundary.

The SIMPLEC scheme algorithm is used for the pressure-velocity coupling, and second-order discretization schemes are applied for the convective and viscous terms and for the turbulence model equations (Ramponi and Blocken, 2012).

Each streamwise gradient is calculated as the difference between the input profile with the corresponding incidence profile at the body position without the building present (Blocken et al., 2007a,b). The velocity streamwise gradient is 3%, the turbulence streamwise gradients are 5% in TKE, 9% in TDR and 10% in SDR (Fig. 3). Similar streamwise gradient values of the turbulence profiles are reported in other simulations of natural ventilation in buildings (Blocken et al., 2007b; Ramponi and Blocken, 2012; Blocken, 2015; Castillo and Huelsz, 2017; Castillo et al., 2019).

Three additional meshes are constructed. Mesh 1 is made by coarsening the reference case mesh (mesh 2) with the factor $\sqrt[3]{1/2}$. Mesh 3 is created by refining with the factor of $\sqrt[3]{2}$ on each coordinate direction of mesh 2. Mesh 4 is generated by refining mesh 3 with the same factor. The number of cells are 335,856 cells for mesh 1, 579,246 cells for mesh 2, 1,035,112 cells for mesh 3 and 2,144,658 cells for mesh 4. In Fig. 4, the isometric views of the four meshes are presented. The mesh sensitivity analysis along the line L_x is shown in Fig. 5a, where L_x is a horizontal line in the central plane, at the height of the middle of the openings. For the sensitivity analysis, the values of velocity from mesh 2 are used as reference. The difference for mesh 1 is 23%, for mesh 3 is 3% and for mesh 4 is 6%. The grid convergence index (GCI) calculation (Roche, 1994) is applied, obtaining an average value of 6% between mesh 2 and mesh 3. The sensitivity analysis confirms that mesh 2 (reference case) provides an accurate solution in a short computational time.

Three of the most used turbulence models in natural ventilation studies are selected for the turbulence model sensitivity analysis: the shear-stress transport (SST) k−ω (Menter, 1994), the renormalization group (RNG) k−ε (Yakhot et al., 1992) and the realizable (R) k − ε (Shih et al., 1995). The comparison with experimental results along L_x is shown in Fig. 5b. In the zone of interest defined as the interior of the building, the average difference of velocity between experiment and numerical models are 5% for SST k−ω model, 7% for RNG k−ε model and 10% for R k−ε model. Although the SST k − ω model has the smallest error, in this work the RNG k − ε is selected, due to the convergence behavior, useful in the average of the parameters over the last iterations. Fig. 6 shows a good qualitative agreement of velocity vector fields in the central plane between experimental and numerical results. The RNG k − ε model reproduces the outside sill vortex formed in the corner between the windward opening sill and the ground. The incoming jet has a download component given by the influence of the outside sill vortex, an inside sill vortex between the windward opening sill and the building floor is formed. On the back interior of the building, the upper part forms a vortex while the remaining flow leaves the building through the leeward opening. It is observed that the simulation reproduces the structure and size of the interior vortexes. Thus, this numerical simulation can be considered validated and useful for the study of the age of air.

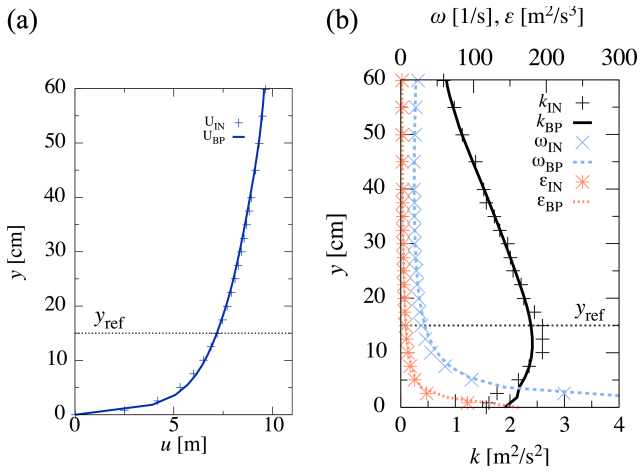

Figure 3: Vertical profiles of: (a) mean velocity *U(y)*; (b) turbulent kinetic energy *k(y)*, turbulent dissipation rate *ε(y)* and specific dissipation rate *ω(y)*. IN and BP subscripts denote the inlet position and the building position, respectively.

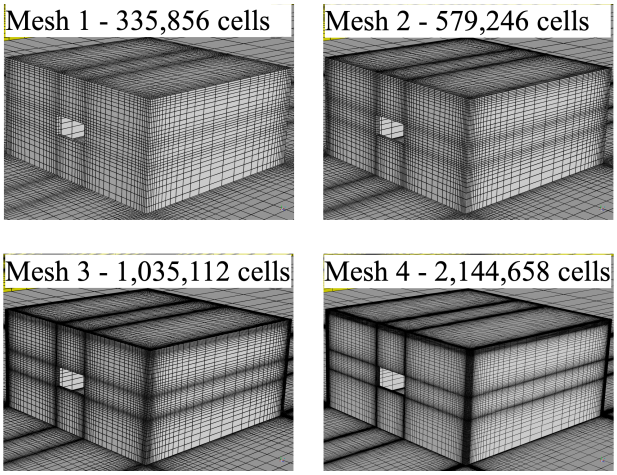

Figure 4: Isometric view of the four meshes: (a) mesh 1 with 335,856 cells; (b) mesh 2 with 579,246 cells (reference case); (c) mesh 3 with 1,035,112 cells; (d) mesh 4 with 2,144,658 cells.

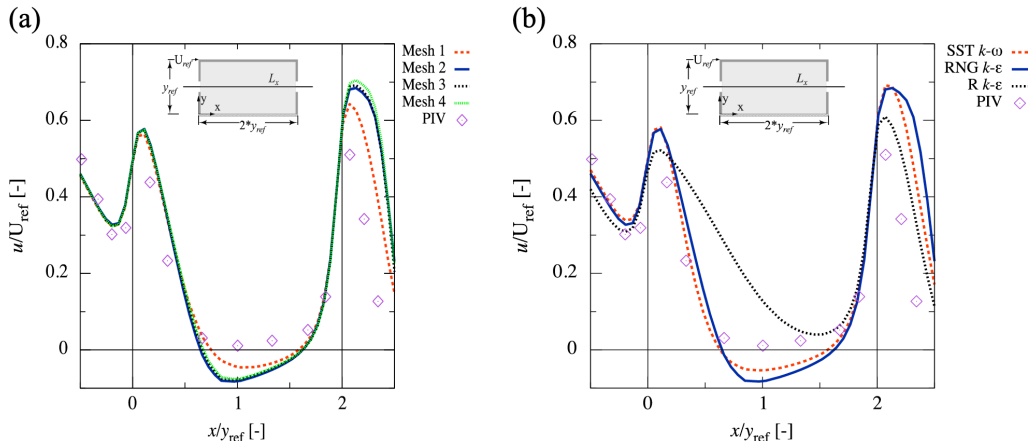

Figure 5: Sensitivity analysis: velocity normalized u/U_{ref} along streamline L_x (a) meshes and experimental results; (b) Turbulence models and experimental results comparison.

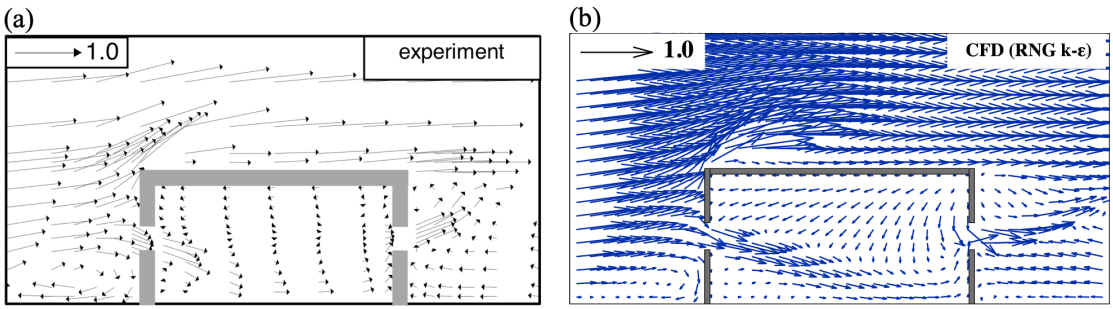

Figure 6: Sensitivity analysis: velocity vector field. (a) experimental result; (b) RNG k − ε model.

AGE OF AIR IMPLEMENTATION ON CFD

When the flow is solved by ANSYS-Fluent, the IDF file "mean_age_diff.c" (ANSYS, 2019) is compiled and used to solve Eq. (2). This IDF file charges the libraries required to calculated the values of the effective diffusion coefficients. For this work, a journal script was created to automatically and systematically implement the age of air calculations (Castillo, 2019).

RESULTS

The age of air study is done using the validated numerical simulation in two scales, model and full. The characteristic time T is calculated using the reference length and velocity $T = y_{ref}/U_{ref}$. It was found that the parameters associated with the age of air normalized with T have the same values at the two scales. The differences of all the normalized parameters associated with the age of air between scales are below 1%. Then, the scaling method between either scale results can be obtained by

$$\frac{\tau_f}{T_f} = \frac{\tau_m}{T_m} \tag{9}$$

where the subscript f and m denote full scale and model scale, respectively. In Table 1, the results for both scales are presented.

Table 1. Results of parameters associated with the age of air for model and full scale.

	Model scale	Full scale
Nominal time τ_n [s]	2.0	447.4
Spatial average of age of air $\langle \tau_i \rangle$ [s]	2.3	514.5
Spatial average of residence time $\langle \tau_i \rangle$ [s]	4.6	1029.0
Efficiency ventilation ϵ [%]	43.5	43.5

At full scale, $I = 2.25 \times 10^{-3}$ s^{-1} that corresponds to 8 air changes per hour. $\langle \tau_r \rangle = 1029.0$ s represents that every 17 min, the air volume in the building is renewed, this implies that the interior building air volume is renewed 3.5 times in an hour, a quantity smaller than the calculated air changes per hour.

Figure 7 shows the contour plots of velocity magnitude and of $\overline{\tau_i}$ in the vertical central plane. The smallest values of $\overline{\tau_i}$ are obtained in the jet from the windward opening. Above this incoming jet in the upper vortex, it is observed $\overline{\tau_i}$ values around 400 s and larger values of $\overline{\tau_i}$ in the inside sill vortex. Figure 8 shows the same contour plots in the horizontal central plane. The smallest values of $\overline{\tau_i}$ are in the windward opening and it is observed $\overline{\tau_i}$ around 400 s in the back side of the building. The greatest values of $\overline{\tau_i}$ are obtained in the vortex zones closed to the front side of the building.

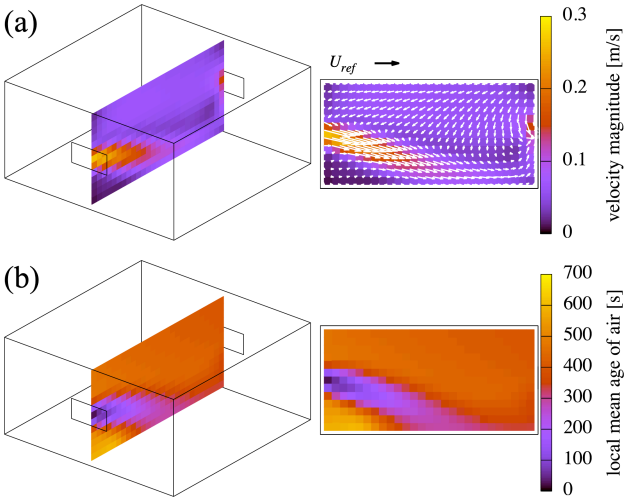

Figure 7. Contour plot in vertical central plane:
(a) velocity magnitude [m/s]; (b) local mean age of air [s]

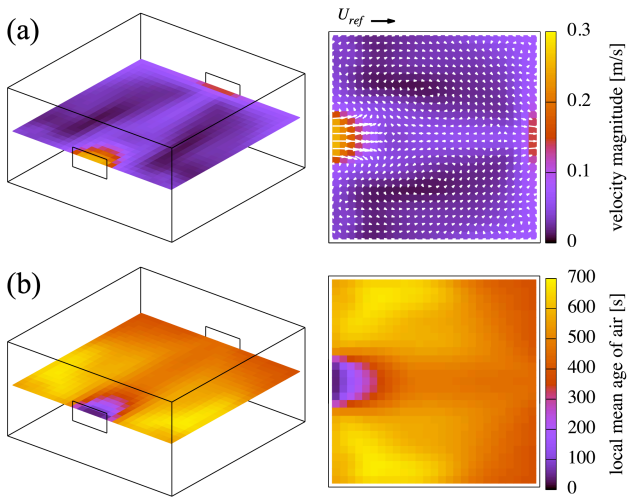

Figure 8. Contour plot in horizontal central plane:
(a) velocity magnitude [m/s]; (b) local mean age of air [s]

CONCLUSIONS

In this paper, the age of air theory and its implementation to a case of a building with natural cross-ventilation, using CFD simulations is presented.

The parameter air exchange rate I only takes into account the interior air volume and the flow across the exhaust. This consideration supposes that the ventilation in the building is an ideal piston flow where the spatial average residence time $\langle \tau_r \rangle$ is equal to the nominal time constant τ_n (Eq. 5). The calculation of the number of building air volume renovation per time unit using $\langle \tau_r \rangle$ results in a more realistic evaluation parameter than the parameter air changes per hour (the inverse of I) .

In a real building (full scale), the evaluation of the natural ventilation with the parameters associated with the age of air can be achieved by scaling the results obtained from model scale experiments or simulations using the characteristic time.

The local mean age of air increases in the vortex zones and stagnation points, while it reduces in the incoming jet.

ACKNOWLEDGMENTS

This work has partially supported by PAPIIT-UNAM IN109519 and CONACYT-SENER 291600 projects. S. Díaz-Calderón acknowledges the scholarship 639370 grant by CONACYT-SENER. J.A. Castillo acknowledges the postdoctoral fellowship grant by the CONACYT-SENER 291600 project.

REFERENCES

ANSYS (2019). *ANSYS FLUENT user's guide*. ANSYS Inc, Canonsburg, Pensilvania, EUA.

ASHRAE (2005) *ASHRAE Handbook Fundamentals*, Si Edition, AmericanSociety of Heating, Refrigerating and Air Conditioning Engineers, Atlanta, GA, 2005.

Blocken, B. (2015). Computational fluid dynamics for urban physics: Importance, scales, possibilities, limitations and ten tips and tricks towards accurate and reliable simulations. *Building and Environment*, 91:219 – 245.

Blocken, B., Carmeliet, J., and Stathopoulos, T. (2007a). CFD evaluation of wind speed conditions in passages between parallel buildings—effect of wall-function roughness modifications for the atmospheric boundary layer flow. *Journal of Wind Engineering and Industrial Aerodynamics*, 95(9):941 – 962.

Blocken, B., Stathopoulos, T., and Carmeliet, J. (2007b). CFD simulation of the atmospheric boundary layer: wall function problems. *Atmospheric Environment*, 41(2):238 – 252.

Castillo, J. A. (2019). Class notes: First steps in Fluent 19.0. http:www.gee.ier.unam.mx/jacat/notes.

Castillo, J. A. and Huelsz, G. (2017). A methodology to evaluate the indoor natural ventilation in hot climates: Heat balance index. *Building and Environment*, 114:366 – 373.

Castillo, J. A., Huelsz, G., van Hooff, T., and Blocken, B. (2019). Natural ventilation of an isolated generic building with a windward window and different windexchangers: CFD validation, sensitivity study and performance analysis. *Building Simulation,* 12(3):475-488.

Cebeci, T. and Bradshaw, P. (1977). *Momentum transfer in boundary layers*.

Etheridge, D. and Sandberg, M. (1996). *Building ventilation: Theory and Measurements*. John Wiley & Suns, United Kingdom.

Jin, R., Hang, J., Liu, S., Wei, J., Liu, Y., Xie, J., and Sandberg, M. (2016). Numerical investigation of wind-driven natural ventilation performance in a multi-storey hospital by coupling indoor and outdoor airflow. *Indoor and Built Environment*, 25(8):1226–1247.

Kurabuchi, T., Ohba, M., Endo, T., Akamine, Y., and Nakayama, F. (2004). Local dynamic similarity model of cross-ventilation part 1 - theoretical framework. *International Journal of Ventilation*, 2(4):371–382.

Launder, B. and Spalding, D. (1974). The numerical computation of turbulent flows. *Computer Methods in Applied Mechanics and Engineering*, 3(2):269 – 289.

Menter, F. (1994). Two-equation eddy-viscosity turbulence models for engineering applications. *AIAA Journal*, 32:1598–1605.

Montazeri, H. and Montazeri, F. (2018). CFD simulation of cross-ventilation in buildings using rooftop wind-catchers: Impact of outlet openings. *Renewable Energy*, 118:502 – 520.

Moonen, P., Defraeye, T., Dorer, V., Blocken, B., and Carmeliet, J. (2012). Urban physics: Effect of the micro-climate on comfort, health and energy demand. *Frontiers of Architectural Research*, 1(3):197 – 228.

Ramponi, R. and Blocken, B. (2012). CFD simulation of cross-ventilation for a generic isolated building: Impact of computational parameters. *Building and Environment*, 53:34 – 48.

Roache, P. J. (1994). Perspective: A method for uniform reporting of grid refinement studies. *Journal of Fluids Engineering*, 116(3): 405–413.

Tominaga, Y., Mochida, A., Yoshie, R., Kataoka, H., Nozu, T., Yoshikawa, M., and Shirasawa, T. (2008). AIJ guidelines for practical applications of CFD to pedestrian wind environment around buildings. *Journal of Wind Engineering and Industrial Aerodynamics*, 96(10):1749 – 1761.

van Hooff, T. and Blocken, B. (2010). Coupled urban wind flow and in- door natural ventilation modelling on a high-resolution grid: A case study for the Amsterdam arena stadium. *Environmental Modelling & Software*, 25(1):51 – 65.

Yakhot, V., Orszag, S. A., Thangam, S., Gatski, T. B., and Speziale, C. G. (1992). Development of turbulence models for shear flows by a double expansion technique. *Physics of Fluids A: Fluid Dynamics*, 4(7):1510– 1520.